

## Thermal stability of superhydrophobic, nanostructured surfaces

Sung-Chul Cha<sup>a,1</sup>, Eun Kyu Her<sup>b,c,1</sup>, Tae-Jun Ko<sup>b,c</sup>, Seong Jin Kim<sup>b</sup>, Hyunchul Roh<sup>c</sup>, Kwang-Ryeol Lee<sup>b</sup>,  
Kyu Hwan Oh<sup>c</sup>, Myoung-Woon Moon<sup>b,\*</sup>

<sup>a</sup> Advanced Functional Materials Research Team, Automotive, Corporate R&D Division, Hyundai Motor Group, Republic of Korea

<sup>b</sup> Institute for Multidisciplinary Convergence of Matters, Korea Institute of Science and Technology, Seoul 136-791, Republic of Korea

<sup>c</sup> Department of Materials Science and Engineering, Seoul National University, Seoul 151-742, Republic of Korea

### ARTICLE INFO

#### Article history:

Received 31 July 2012

Accepted 24 September 2012

Available online 2 October 2012

#### Keywords:

Superhydrophobicity

Nanostructure

Thermal stability

Wetting transition

### ABSTRACT

The thermal stability of superhydrophobic, nanostructured surfaces after thermal annealing was explored. Flat surfaces coated with hydrophobic diamond-like carbon (DLC) via plasma polymerization of hexamethyldisiloxane (HMDSO) showed a gradual decrease in the water contact angle from 90° to 60° while nanostructured surfaces maintained superhydrophobicity with more than 150° for annealing temperatures between 25 and 300 °C. It was also found that surfaces with nanostructures having an aspect ratio of more than 5.2 may maintain superhydrophobicity for annealing temperatures as high as 350 °C; above this temperature, however, the hydrophobicity on surfaces with lower aspect ratio nanostructures gradually degraded. It was observed that regardless of the aspect ratios of the nanostructure, all superhydrophobic surfaces became superhydrophilic after annealing at temperatures higher than 500 °C.

© 2012 Elsevier Inc. All rights reserved.

### 1. Introduction

Functional hard coating materials have been developed to satisfy harsh requirements, such as low friction, wear resistance, sticking resistance, and high temperature stability up to 300 °C [1,2]. Stable hydrophobicity has been considered a crucial property of coating materials especially due to the recent demand for high temperature performance in various applications, such as automobile parts or cooking wares. There have been reports of hydrocarbon materials being used as hydrophobic coatings with lower surface energy, comparable to that of polytetrafluoroethylene (PTFE), and with good mechanical performance in terms of wear resistance, low friction, and hardness [3,4]. To lower the surface energy for hydrophobic coatings, chemical modifications of carbon films have been performed by adding a third element, such as Si–O, Si, or F, into an amorphous carbon matrix, resulting in a surface energy as low as 20 mN/m [3–5]. However, the hydrophobicity of these low-energy surfaces with Si–O contained within the hydrocarbon coating was reported to decrease gradually as the annealing temperature increased above 250 °C [3]. It was reported that hydrogen might be debonded from the hydrogen–carbon bonding interactions approximately 260 °C [5] and induce significant degradation of the hydrophobic properties in hydrocarbon coatings.

Hydrophobic or superhydrophobic surfaces are achieved by applying coatings with low surface energy on textured surfaces,

which usually mimics micro-/nano- or hybrid-structures, such as that of the lotus leaf with high water contact angle (CA) and low contact angle hysteresis (CAH) [6]. When a water droplet is released onto a lotus leaf, it forms a nearly perfect spherical shape that rolls off and cleans the contaminated surfaces. This water-repellent behavior is attributed to the leaf surface structure due to its micro-/nano-hierarchy and relatively hydrophobic epicuticular wax crystalloid coating [7,8]. This indicates that surface texturing is also essential for high hydrophobicity, in addition to the low surface energy of materials with hydrophobic coatings. Until now, there have been many studies on the wetting and kinetics of droplet behavior on superhydrophobic surfaces [9,10] but few studies on the thermal stability of the superhydrophobicity of structured surfaces. Saleema and Farzaneh reported that the superhydrophobicity of ZnO nanotower structures with stearic acid modifications was degraded at certain temperatures due to desorption of hydrophobic stearic acid [11]. However, the work did not discuss in detail the contribution of nanostructure to the thermal stability of the superhydrophobic surfaces by varying its geometric configuration.

In this work, the thermal stability of hydrophobicity and superhydrophobicity was investigated on nanostructured surfaces with different geometries. We used a nanostructured Si wafer coated with a hydrophobic coating of a diamond-like carbon (DLC) with and without Si–O and annealed at temperatures ranging from ambient temperature to 500 °C. Due to the geometric aspect ratio, defined as a ratio of the height over the diameter of a nanopillar structure, superhydrophobic, nanostructured surfaces maintained their hydrophobicity with CAs of 150° and low CAH at temperatures up to 350 °C; above which temperature, the wettability

\* Corresponding author.

E-mail address: mwmoon@kist.re.kr (M.-W. Moon).

<sup>1</sup> These authors contributed equally to this work.

suddenly transitioned from hydrophobic or superhydrophobic to superhydrophilic due to thermal degradation of the hydrocarbon coating. Several methods have been suggested for increasing the hydrophobicity of surfaces, mainly involving micro- or nano-scale structures coated with low surface energy materials [12–14]. Among these methods, plasma treatment using a dry etching technique is considered an important method for fabrication of nanopillar structures and subsequent hydrophobic coatings for hydrophobic surfaces [15]. On flat and nanostructured surfaces, Si-O<sub>x</sub>-containing DLC (SiO<sub>x</sub>-DLC) films were coated via plasma polymerization of a hexamethyldisiloxane (HMDSO) vapor. SiO<sub>x</sub>-DLC films were used as hydrophobic coatings comparable to PTFE with lower surface energy than that of the substrate and with good mechanical performance in terms of wear resistance, hardness, and controllable coating thickness [3]. To compare the thermal degradation behavior of superhydrophobic surfaces coated with SiO<sub>x</sub>-DLC films, pure DLC films were selected for coating onto flat and nanostructured surfaces. The thermal stability was determined by measuring the static CA and the CAH of water droplets on annealed hydrophobic surfaces with different geometric aspect ratios.

## 2. Experimental methods

### 2.1. Preparation of sample surfaces

Two Si (100) surfaces with different roughnesses were prepared: single rough Si surfaces with nanopillars and flat, bare Si wafers. Si wafers were etched to form the nanopillars using radio frequency (r.f.) glow discharge of CF<sub>4</sub> gas at 30 mTorr and –600 V of bias voltage [15]. This simple etching procedure produced nanopillars on the Si surface without forming a mask caused by the local deposition of carbon films from the CF<sub>4</sub> gas (a self-masking effect) and the preferred etching of Si with the F atoms [16,17], which have high reactivity toward Si [18]. CF<sub>4</sub> plasma treatment duration ranging from 5 to 60 min was chosen to give the desired roughness or solid fraction of the surfaces [15]. Scanning electron microscopy (SEM, Nova NanoSEM 200, FEI) was used for the observation of nanostructures formed on the sample surfaces.

### 2.2. Hydrophobic coatings

To prepare the DLC surfaces, SiO<sub>x</sub>-DLC films and pure DLC (or a-C:H) films were deposited using HMDSO and CH<sub>4</sub> gases, respectively, via r.f. plasma-assisted chemical vapor deposition (PACVD). The SiO<sub>x</sub>-DLC film from the plasma polymerization of HMDSO was chosen to increase the surface hydrophobicity due to its low surface energy of 24.2 mN/m compared with 43.8 mN/m for a pure DLC film [3,19]. The bias voltage was fixed at –400 V and 1.33 Pa for 10 s, which resulted in a static CA of 90° for the SiO<sub>x</sub>-DLC films and 70° for the pure DLC films on flat surfaces; on flat surface, while on nanostructured surfaces, the CA was close to 155° for the SiO<sub>x</sub>-DLC films and 100° for the pure DLC films. The details and processes used in the fabrication of superhydrophobic surfaces were implemented from previous works [15,16,20–22].

### 2.3. Thermal annealing and contact angle measurement

Thermal annealing was performed in a furnace in an ambient environment. First, the furnace was heated to the desired annealing temperature, up to 500 °C, for 60 min; the samples were then inserted into the furnace. After annealing for 24 h, the samples were taken out of the hot furnace and cooled down to room temperature in less than 60 min. The water CA was measured by analyzing images of a deionized (D.I.) sessile water droplet on each

surface taken with a CCD camera (Olympus – DP 71). The 5-μL water droplets generated with a syringe gently landed on the prepared surfaces. Measurement of the dynamic CA was performed with the dynamic sessile drop method, which measures the dynamic CA by slowly changing the volume of sessile water drops. The reported CAs were an average of measurements from five different spots on each sample. The critical advancing CA was measured by increasing the drop volume with an aid of a syringe needle immersed in the drop until the contact line started to move; similarly, the receding CA was measured by decreasing the drop volume until the contact line started to move. The difference between the critical advancing CA and receding CA corresponds to the CAH.

## 3. Results and discussion

As the annealing temperature increased up to 400 °C, the hydrophobicity was tracked by measuring the water CA of the pure DLC films on flat substrates and rapidly decreased from 70° to 10°. On a bare Si wafer, a CA greater than 30° was maintained, indicating the chemical stability of SiO<sub>2</sub> over the annealing temperature range shown in Fig. 1. For the SiO<sub>x</sub>-DLC film-coated, flat Si surface, the initially high CA of approximately 90° gradually decreased to 65° as the annealing temperature increased up to 400 °C and suddenly decreased to less than 23° at 500 °C. This result is consistent with a previous report that the stability of a hydrophobic coating containing hydrogen bonds is affected by the breakage of hydrogen-carbon bonds at approximately 300 °C, resulting in a loss of hydrophobicity [5].

Fig. 2 shows micrographs of the morphologies of nanostructured surfaces coated with pure DLC and SiO<sub>x</sub>-DLC, the geometries of which consisted of nanopillars fixed in diameter and height that were formed after 60 min of CF<sub>4</sub> plasma treatment and subsequent deposition of a 10-nm thick coating for each type of DLC. The CA changed dramatically from 100° to 20° on the nanostructured surfaces with a pure DLC coating while increasing the annealing temperature from 100 °C to 300 °C; the CA of approximately 155° was almost unchanged on the nanostructured surfaces coated with a SiO<sub>x</sub>-DLC film, as shown in the inset images of a droplet on each surface.

The behavior of the water CAs on sample surfaces prepared with different morphologies and on different surface coatings were explored, as shown in Fig. 3. The CAs for as-prepared samples with flat Si surfaces with SiO<sub>x</sub>-DLC coatings and pure DLC coatings were measured as 90° and 65°, respectively; the CA increased to 155° for the nanostructured Si surfaces with SiO<sub>x</sub>-DLC coatings and to 100°

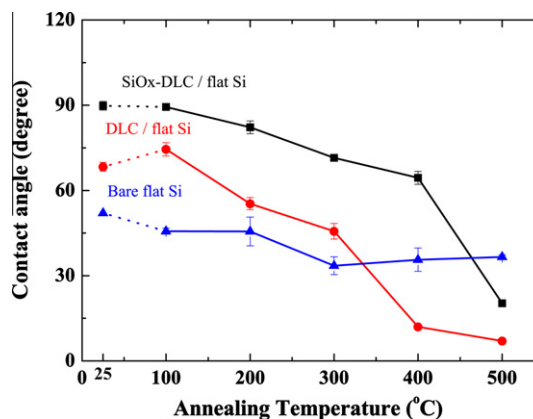
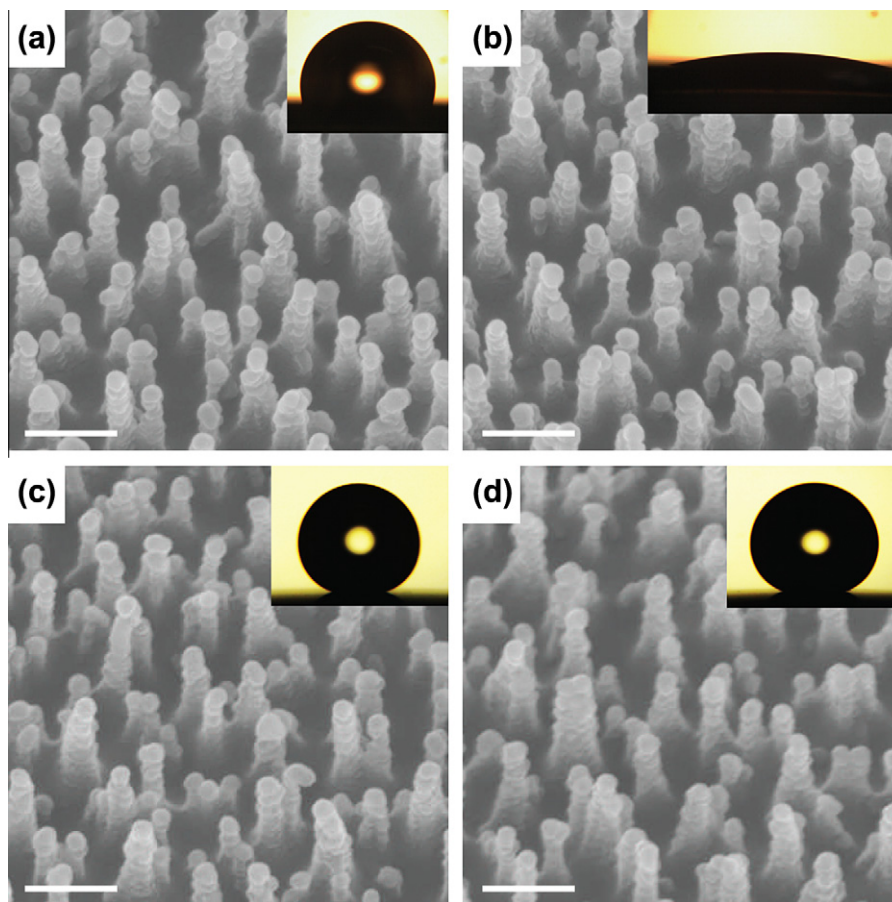
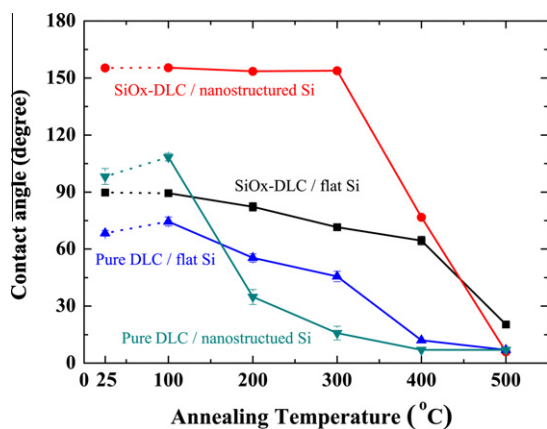


Fig. 1. Measured values of water CAs on various surfaces with annealing temperature.



**Fig. 2.** SEM micrographs of nanostructured Si wafers at (a) 100 °C and (b) 300 °C for the pure DLC coating, and (c) 100 °C and (d) 300 °C for the SiO<sub>x</sub>-DLC coating. All SEM micrographs were taken at a 30° tilting angle view. Scale bars are 300 nm. Insets are optical micrographs of a water droplet on each of the treated surfaces.



**Fig. 3.** Water CAs on nanostructured and flat surfaces coated with SiO<sub>x</sub>-DLC and pure DLC were measured at several annealing temperatures.

for the nanostructured Si surfaces with pure DLC coatings. As the annealing temperature increased, the CAs gradually decreased on the flat surfaces. For the nanostructured surfaces with pure DLC coatings, however, after a slight increase in CA to 115° at 100 °C, the CAs sharply decreased with temperature. However, the CA on the nanostructured Si surfaces with SiO<sub>x</sub>-DLC coatings remained greater than 150° for temperatures up to 300 °C; above this temperature, the CA decreased to less than 10° at 500 °C. This transition in hydrophobicity is explained by a wetting transition from a

Cassie–Baxter state to a Wenzel state on the structured surfaces, as explained below.

To explain the wetting transition on nanostructured surfaces, a previous simple theory was adopted based on the transition from a Cassie–Baxter state to a Wenzel state. Because the surface roughness and solid fraction were calculated as a function of the geometrical parameters of nanopillars at interfacial energy equilibrium including the diameter, height, and spacing length between the pillars, Young's equation [6] is given by  $\cos \theta = \frac{\gamma_{SG} - \gamma_{SL}}{\gamma_{LG}}$ , where interface energies for solid (S)/gas (G) are  $\gamma_{SG}$ ; liquid (L)/gas (G),  $\gamma_{LG}$ ; and liquid (L)/solid (S),  $\gamma_{SL}$ . When a droplet completely wets a rough surface with roughness  $r$ , the apparent CA,  $\theta_w$ , is given as a function of  $r$  and  $\theta$ :

$$\cos \theta_w = r \cos \theta, \quad (1)$$

where  $\theta$  is the static CA on the flat surfaces. However, when a droplet partially wets the top of the pillars and when perfect wetting is resisted by air trapped between the pillars in the Cassie–Baxter regime [6], the apparent CA,  $\theta_{CB}$ , is given as a function of the roughness fraction,  $f_s$ , and the static CA,  $\theta$ :

$$\cos \theta_{CB} = f_s (\cos \theta + 1) - 1. \quad (2)$$

Here, as the surface roughness increases, the apparent CA would also increase in the Cassie–Baxter state. The CAs increased on as-prepared SiO<sub>x</sub>-DLC-coated nanostructured surfaces prior to thermal annealing because the wettability follows the Cassie–Baxter relationship due to the hydrophobic nature of the SiO<sub>x</sub>-DLC coating (CA ~90°) as well as the higher roughness fraction. As the annealing temperature increased, the hydrophobic property of the

$\text{SiO}_x$ -DLC coating on flat surfaces decreased to  $75^\circ$  due to degradation of the C–H networks and Si–O bonds [5,23]. However, experimental results for the CAs on  $\text{SiO}_x$ -DLC-coated nanostructured surfaces showed that the surfaces remained in the superhydrophobic state for annealing temperatures up to  $300^\circ\text{C}$ , which indicates that Eq. (2) is still valid for a CA of  $\sim 75^\circ$  on a flat substrate annealed at  $300^\circ\text{C}$  because it leads to  $\theta_{CB} \sim 150^\circ$  on a nanostructured hydrophobic surface. However, for annealing temperatures of  $400^\circ\text{C}$  and  $500^\circ\text{C}$ , the CAs decreased sharply to less than  $80^\circ$  and  $10^\circ$ , respectively, on the nanostructured surfaces, whereas the CAs on the flat surfaces decreased to  $65^\circ$  and  $20^\circ$ , respectively. This phenomenon on the nanostructured surfaces indicates a transition to the Wenzel regime because there is insufficient surface hydrophobicity to maintain the Cassie–Baxter state, which means that the gaps that occur between nanostructures are filled with water because the solid–water interface becomes more energetically favorable than the solid–air interface at high annealing temperatures. Therefore, the bottom of the water droplet has conformal contact with the solid surface. Such conformal contact

between solid and water dramatically increases the solid–water interfacial force on hydrophilic surface and causes a sudden reduction in CA, both of which are predicted by the Wenzel equation [6,7].

Another experiment on the effect of different etching times during the  $\text{CF}_4$  plasma treatment was performed, and the surface morphologies of the nanostructures produced with variations in the geometrical aspect ratio are shown in Fig. 4. It was reported that the increase in the aspect ratio of Si nanopillars would be induced by self-mask behavior of the local deposition of fluorocarbon clusters formed on Si surface during  $\text{CF}_4$  plasma etching [16]. Local fluorocarbon clusters formed from  $\text{CF}_x$  ions would suppress etching on Si, while the unmasked areas are continuously etched, resulting in the increase in the aspect ratio of the Si nanostructures as shown in Fig. 4a. Previous studies reported that nanostructures with relatively higher aspect ratios were formed after 20 min of  $\text{CF}_4$  treatment on a Si wafer [13,14]. The aspect ratio of the nanostructure was measured for  $\text{CF}_4$  treatment duration of 20 min, 30 min, 60 min, and 90 min, resulting in average aspect ratios of 2.9, 3.7, 5.2, and 8.0, respectively. Fig. 5a shows the wettability with

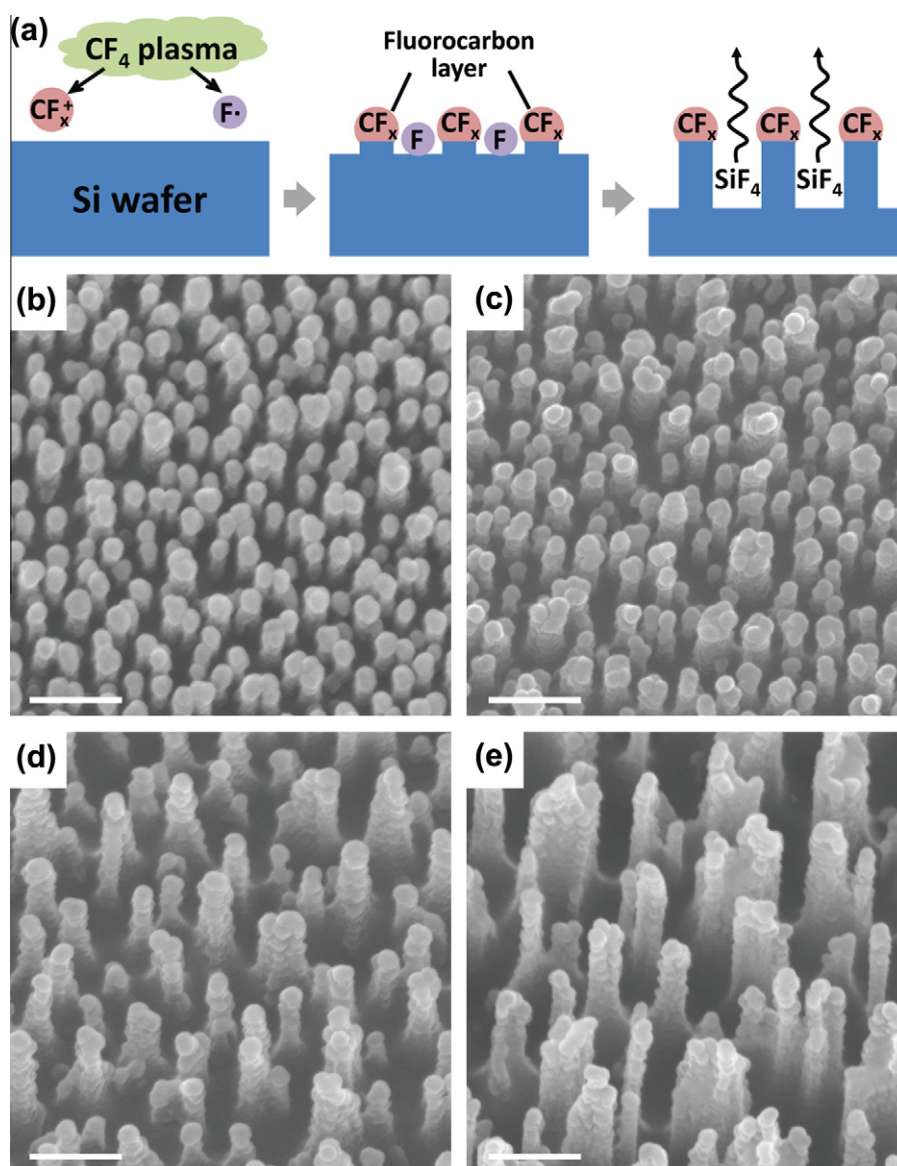


**Fig. 4.** (a) A schematic about the aspect ratio increasing on Si nanopillars with the increase of  $\text{CF}_4$  etching duration and SEM micrographs taken at a  $30^\circ$  tilting angle view of nanostructured surfaces with different  $\text{CF}_4$  plasma treatment duration; (b) 20 min, (c) 30 min, (d) 60 min, and (e) 90 min. Scale bars are 300 nm.

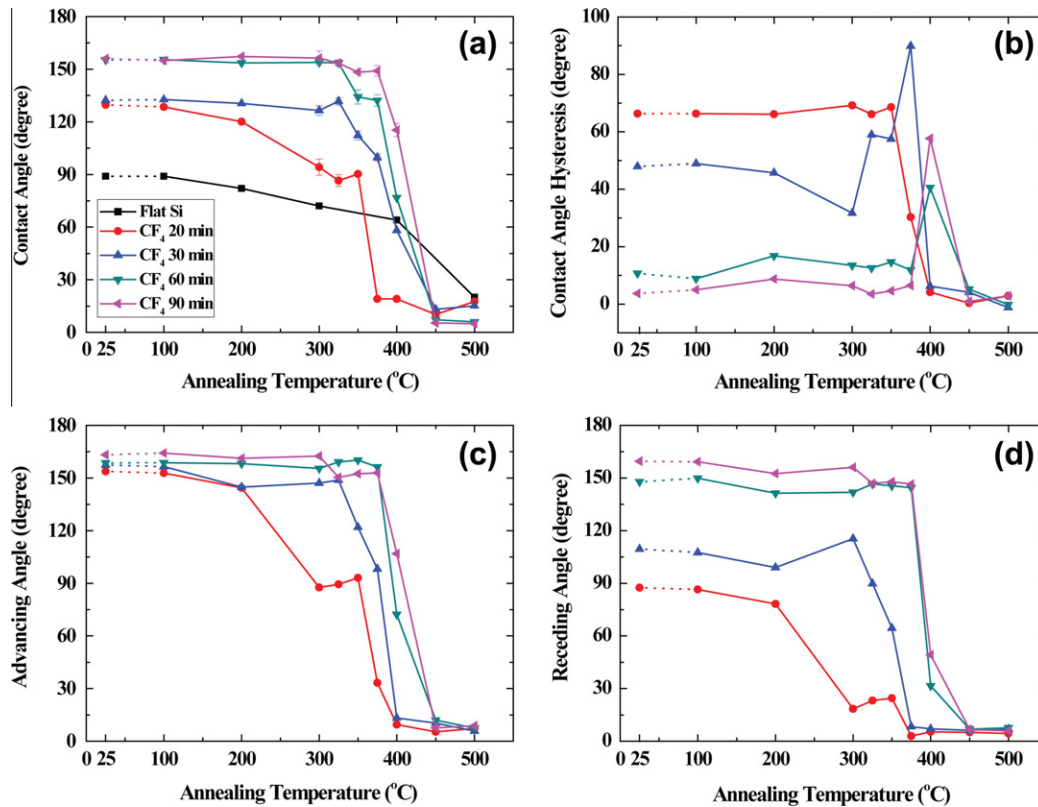


**Fig. 5.** (a) Water CA measurements in static water drop and (b) CAH measurements; the CAH measurements are estimated by the difference between the (c) advancing and (d) receding CAs on the nanostructured surfaces formed with various CF<sub>4</sub> plasma treatment duration.

different aspect ratio values for various thermal annealing temperatures on nanostructured surfaces. While the water CA decreased on flat surfaces with increasing annealing temperature, nanostructured surfaces had stable hydrophobic behavior by maintaining a CA greater than 150°, except for the two surfaces that had undergone 20 min and 30 min of CF<sub>4</sub> plasma treatment. This result indicates that the SiO<sub>x</sub>-DLC coating on nanostructured surfaces with an aspect ratio greater than 5.2 may maintain superhydrophobicity for annealing temperatures as high as 350 °C. In contrast, the water CA on a flat surface drops below 75° at 300 °C, which means that the surface is no longer hydrophobic. When annealed above 450 °C, nanostructured surfaces coated with SiO<sub>x</sub>-DLC became superhydrophilic, regardless of the aspect ratio. In addition, Fig. 5b shows the CAH measurement, which is estimated from the difference between advancing (Fig. 5c) and receding (Fig. 5d) angles on the same specimens. Low CAH is indicated by the case with which a water drop would roll off of a surface, in accordance with the receding angle. CAH and the receding angle were maintained a low value of approximately 15° and a high value of approximately 150°, respectively, on the nanostructured surfaces for 60 min and 90 min treated by CF<sub>4</sub> plasma up to 350 °C; above this temperature, the CA and receding angle suddenly decreased. This result clearly shows the degradation of the Cassie–Baxter state for nanostructured surfaces at higher annealing temperatures [6]. For the nanostructured surfaces that had undergone 20 min and 30 min of CF<sub>4</sub> plasma treatment, the CAHs were relatively higher than for other cases at lower annealing temperature in which the receding angles were quite lower than the advancing angles due to lower aspect ratios of the nanostructures [22]. However, the receding and advancing angles became less than 10° for annealing temperatures greater than 400 °C.

#### 4. Conclusion

The thermal stability of nanostructured superhydrophobic surfaces was investigated after annealing at up to 500 °C. It was found that neither SiO<sub>x</sub>-DLC nor pure DLC coatings on flat surfaces could overcome the thermal degradation of wettability due to degradation of hydrogen-carbon bonds approximately 350 °C as the annealing temperature increased. However, for nanostructured surfaces coated with SiO<sub>x</sub>-DLC, the CA remained at 155° as the annealing temperature increased up to 350 °C, indicating stable superhydrophobicity, but the water CA abruptly decreased below 10° at annealing temperatures of 450 °C or higher, showing superhydrophilicity. Furthermore, receding and advancing angles on the nanostructured, superhydrophobic surface slightly decreased from 150° for annealing temperatures below 350 °C; above 450 °C, however, the CAs became less than 15°. The morphological aspect ratios of the nanostructure formed by CF<sub>4</sub> plasma treatment played a crucial role in sustaining superhydrophobicity. The superhydrophobic surfaces with nanostructures having an aspect ratio greater than 5.2 maintain superhydrophobicity for annealing temperatures as high as 350 °C, with a CA greater than 150° and a CAH lower than 15°, although the water CA on a flat surface drops below 75° at 350 °C. When annealed above 450 °C, nanostructured surfaces coated with SiO<sub>x</sub>-DLC became superhydrophilic regardless of the aspect ratio of the nanopillars.

It can be suggested that because surface texturing or nanostructuring may improve the thermal stability of superhydrophobicity, superhydrophobic surfaces tuned by choosing appropriate coating materials and aspect ratios of surface features could be useful in various applications required for thermal stability, such as automobile engine parts or cooking wares.

## Acknowledgments

This study was financially supported in part by a project from the Fundamental R&D Program for Core Technology of Materials, a project from the MKE (10040003) (MWM), a KIST internal project, and by the National Research Foundation of Korea (NRF) through the Ministry of Education, Science and Technology (R11-2005-065, KHO).

## References

- [1] K. Bewilogua, G. Brauer, A. Dietz, J. Gabler, G. Goch, B. Karpuschewski, B. Szyszka, *CIRP Ann.-Manuf. Technol.* 58 (2009) 608.
- [2] H.M. Chung, W.E. Ruther, J.E. Sanecki, A. Hins, N.J. Zaluzec, T.F. Kassner, *J. Nucl. Mater.* 239 (1996) 61.
- [3] M. Grischke, A. Hieke, F. Morgenweck, H. Dimigen, *Diamond Relat. Mater.* 7 (1998) 454.
- [4] J.L. Parker, P.M. Claesson, J.H. Wang, H.K. Yasuda, *Langmuir* 10 (1994) 2766.
- [5] D.R. Tallant, J.E. Parmeter, M.P. Siegal, R.L. Simpson, *Diamond Relat. Mater.* 4 (1995) 191.
- [6] D. Quere, *Ann. Rev. Mater. Res.* 38 (2008) 71.
- [7] C. Ishino, K. Okumura, D. Quere, *Europhys. Lett.* 68 (2004) 419.
- [8] A. Tuteja, W. Choi, M. Ma, J.M. Mabry, S.A. Mazzella, G.C. Rutledge, G.H. McKinley, R.E. Cohen, *Science* 318 (2007) 1618.
- [9] P. Brunet, F. Lapiere, V. Thomy, Y. Coffinier, R. Boukherroub, *Langmuir* 24 (2008) 11203.
- [10] J. Hyväluoma, J. Timonen, *Europhys. Lett.* 83 (2008) 64002.
- [11] N. Saleema, M. Farzaneh, *Appl. Surf. Sci.* 254 (2008) 2690.
- [12] L. Feng, S. Li, Y. Li, H. Li, L. Zhang, J. Zhai, Y. Song, B. Liu, L. Jiang, D. Zhu, *Adv. Mater.* 14 (2002) 1857.
- [13] K. Koch, H.F. Bohn, W. Barthlott, *Langmuir* 25 (2009) 14116.
- [14] N. Zhao, J. Xu, Q.D. Xie, L.H. Weng, X.L. Guo, X.L. Zhang, L.H. Shi, *Macromol. Rapid Commun.* 26 (2005) 1075.
- [15] T.G. Cha, J.W. Yi, M.W. Moon, K.R. Lee, H.Y. Kim, *Langmuir* 26 (2010) 8319.
- [16] T.Y. Kim, B. Ingmar, K. Bewilogua, K.H. Oh, K.R. Lee, *Chem. Phys. Lett.* 436 (2007) 199.
- [17] Y.P. Zhao, J.T. Drotar, G.C. Wang, T.M. Lu, *Phys. Rev. Lett.* 82 (1999) 4882.
- [18] X. Detter, R. Palla, I. Thomas-Boutherin, E. Pargon, G. Cunge, O. Joubert, L. Vallier, *J. Vac. Sci. Technol. B: Microelectron. Nanometer Struct.* 21 (2003) 2174.
- [19] M. Ishihara, T. Kosaka, T. Nakamura, K. Tsugawa, M. Hasegawa, F. Kokai, Y. Koga, *Diamond Relat. Mater.* 15 (2006) 1011.
- [20] E.K. Her, T.-J. Ko, K.-R. Lee, K.H. Oh, M.-W. Moon, *Nanoscale* 4 (2012) 2900.
- [21] Y. Rahmawan, M.W. Moon, K.S. Kim, K.R. Lee, K.Y. Suh, *Langmuir* 26 (2009) 484.
- [22] B. Shin, K.-R. Lee, M.-W. Moon, H.-Y. Kim, *Soft. Matter* 8 (2012) 1817.
- [23] W.J. Wu, M.H. Hon, *Surf. Coat. Technol.* 111 (1999) 134.